



LAB - FLUID SURFACE INTERACTION

BY

SACHIN SRINIVASA SHETTY

Contents

1	Part I:Study of the NACA0012 profile mounted on a vertical spring	3
1.1	Imposed Motion in X-direction	3
1.1.1	Evaluation of the added-mass coefficient	4
1.2	Profile Mounted on a Vertical Spring	4
1.2.1	Case 1 :Solid Density equal to 10 times the fluid density	5
1.2.2	Case 2 :Solid Density equal to 1/2 times the fluid density	8
2	Part II:Use of CFD software for a classical resistance case	12
2.1	Evaluation of Trim,Sinkage and Resistance Coefficient	16
2.1.1	Trim	16
2.1.2	Sinkage	16
2.1.3	Resistance Coefficient(C_T)	17
2.1.4	Analysis of free surface elevation along the hull	18
2.2	Visualisation of flow	18
2.3	Euler vs RANSE simulation	19
2.4	Quasi-static approach vs Resolution of the Newton law	21
3	Part III :Study of a 3D Composite Plate through a modal approach	23
3.1	Lateral deflection of the tip	28

List of Figures

1	Evolution of Forces	3
2	Evolution of Residual	3
3	Kinematics of the body	5
4	Differences in acceleration between non-linear iterations	6
5	Comparison of Forces for with and without special stabilisation	6
6	Comparison of Forces for Rigid and weighting deformation	7
7	Comparison of Rigid and weighting deformation on T_y	7
8	Evolution of forces without any stabilisation procedure	8
9	Evolution of forces with stabilisation procedure	8
10	Evolution of forces for suddenly imposed vertical acceleration	9
11	Evolution of forces	10
12	Evolution of T_y with time	10
13	DTMB case 1.3	12
14	Evolution of Force	13
15	Evolution of M_z	13
16	Evolution of Acceleration	14
17	Evolution of Residual U and V	14
18	Evolution of Residual W	15
19	Evolution of Residual P and K	15
20	Evolution of Trim	16
21	Evolution of Sinkage	17
22	Comparison free surface elevation	18
23	Visualisation of free surface wave elevation	18
24	Evolution of Force	19
25	Evolution of M_z	19

26	Evolution of Acceleration	20
27	Evolution of Force	21
28	Evolution of M_z	21
29	Evolution of Acceleration	22
30	Evolution of F_x	23
31	Evolution of F_x	24
32	Evolution of F_y	24
33	Evolution of F_z	25
34	Evolution of X-displacement	26
35	Evolution of Y-displacement	26
36	Evolution of Z-displacement	27
37	Comparison of Lateral deflection with experimental values	28

List of Tables

1	Estimation of added mass Components	4
2	Comparison of Trim,Sinkage and Resistance coefficient	17

1 Part I: Study of the NACA0012 profile mounted on a vertical spring

In this section, We are going to look into the Classical NACA0012 profile. Firstly, The X-motion is imposed using a classical ramp. The forces, residuals and added mass coefficients are evaluated. Then two cases are studied, In the first case, We choose the solid density being 10 times the fluid density and the second case, we choose a solid density to 1/2 the fluid density.

1.1 Imposed Motion in X-direction

The below figure.1 represents the evolution of the forces in x and y direction.

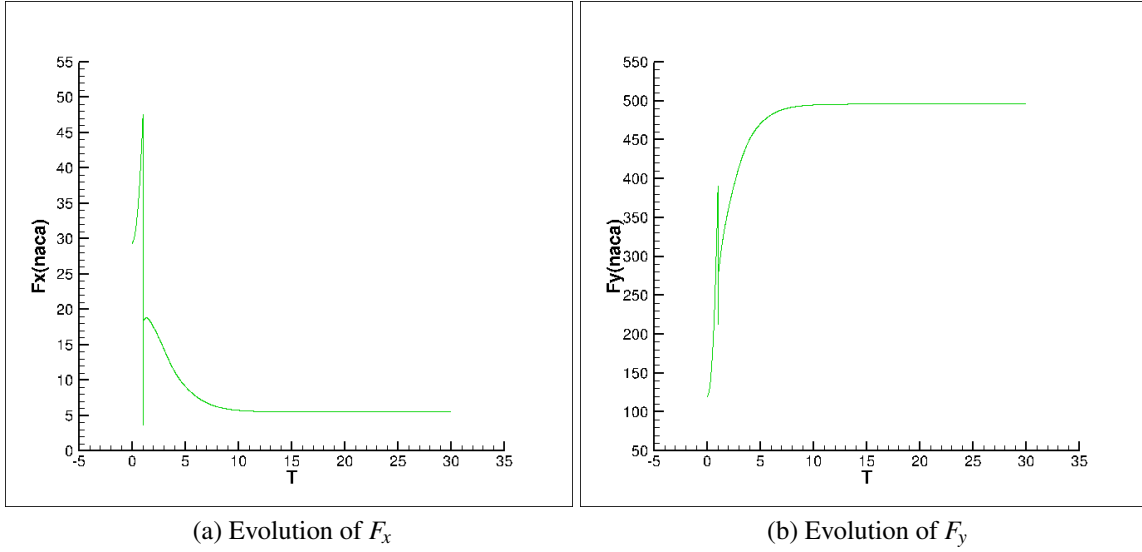


Figure 1: Evolution of Forces

The below figure.2 represents the evolution of the residuals.

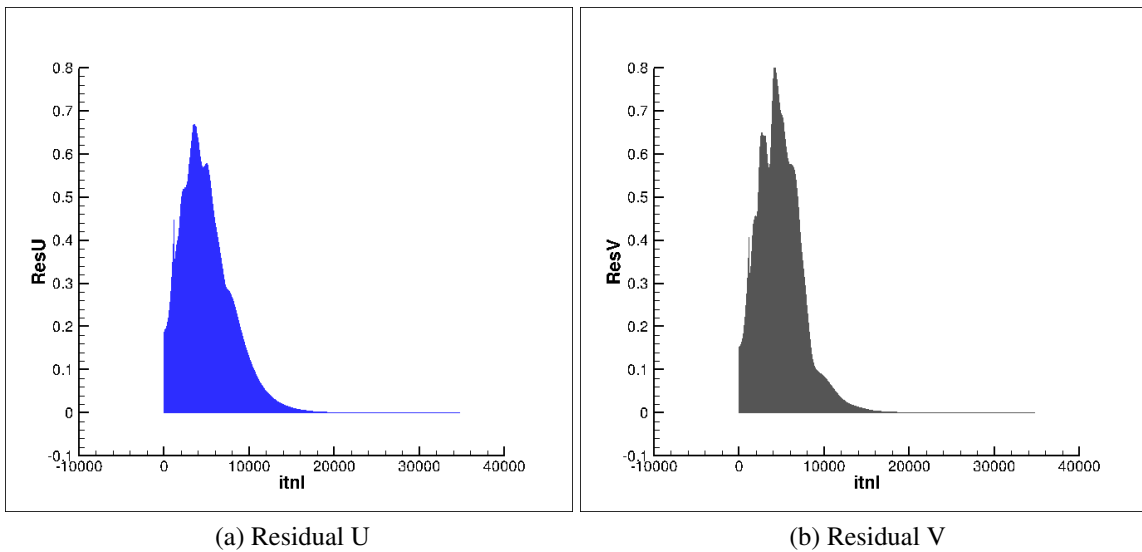


Figure 2: Evolution of Residual

From the figure, we get the added mass term as $M_{xx} = 29.274742$ and $M_{yx} = 119.8158749$.

1.1.1 Evaluation of the added-mass coefficient

We now estimate the added mass by running a simulation where the T_x and T_y motion are solved with 1 time step. The added mass coefficient estimation mode is set to accurate and approximate mode with a frequency 0. The below table shows the values of added mass matrix we obtained. We can observe that the M_{xx} and M_{yx} values computed from the force plots in the earlier computations are in agreement with these results. It can be observed there is a minor difference between an accurate and approximate estimation. So, Approximate mode is enough as it takes much less time to compute the added mass coefficients. Also the $M_{xy} \approx M_{yx}$ are similar and this says that the added mass matrix is symmetric. The gradient reconstruction on the face through a centered approach involves corrective terms which represents the misalignment. The approximate method ignores the corrective terms but the accurate method considers it.

Mode	M_{xx}	M_{yx}	M_{xy}
Accurate	29.4496	120.2299	120.3067
Approximate	29.0220	118.2685	118.2307

Table 1: Estimation of added mass Components

1.2 Profile Mounted on a Vertical Spring

In this section, we are going to define a new computation where the DOF T_y is as solved and also the action of a linear vertical spring is included. The stiffness of the spring is calculated to allow the displacement of $0.25c$, where c is chord of the wing. The value of the convergence force is approximated $F_y = 500N$. Then the stiffness of the spring is calculated as,

$$F_y = k_y * (0.25c)$$

$$k_y = \frac{500}{0.25} = 2000N/m$$

The T_y motion is now solved in the following cases.

1.2.1 Case 1 :Solid Density equal to 10 times the fluid density

In this Case,the volume of the profile is $0.08m^3/m$ and the density of the fluid is $1000kg/m^3$.We get the mass of the wing as $800kg/m$.We run the simulation using a special stabilisation procedure.The below figure,3 shows the kinematics of the wing.It can be observed that the final T_x position is 14.5 as expected.

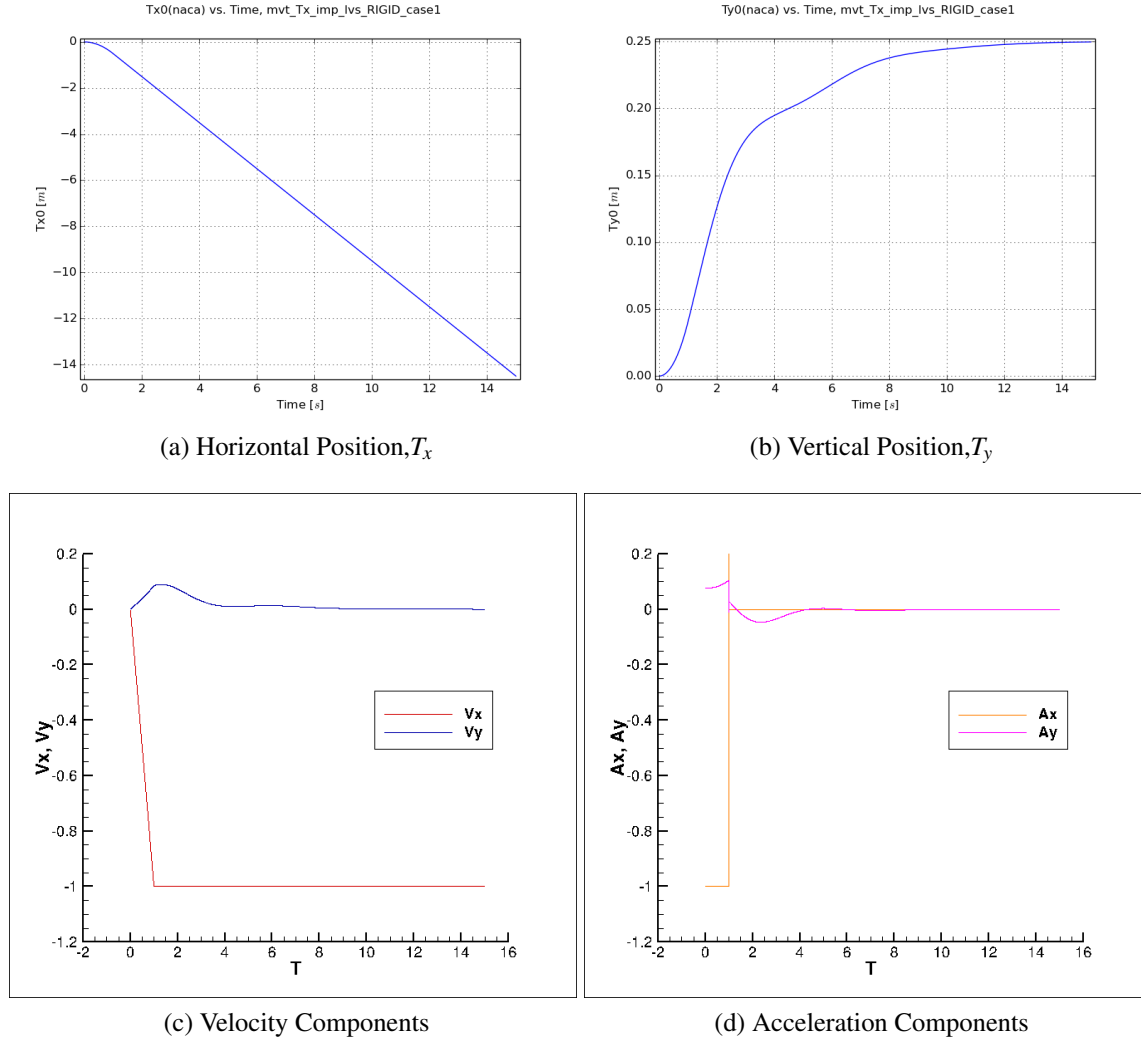


Figure 3: Kinematics of the body

The below figure,4 shows the differences in acceleration between non-linear iterations.It can be observed that the convergence tend to zero,so the stabilisation procedure should not affect the results.

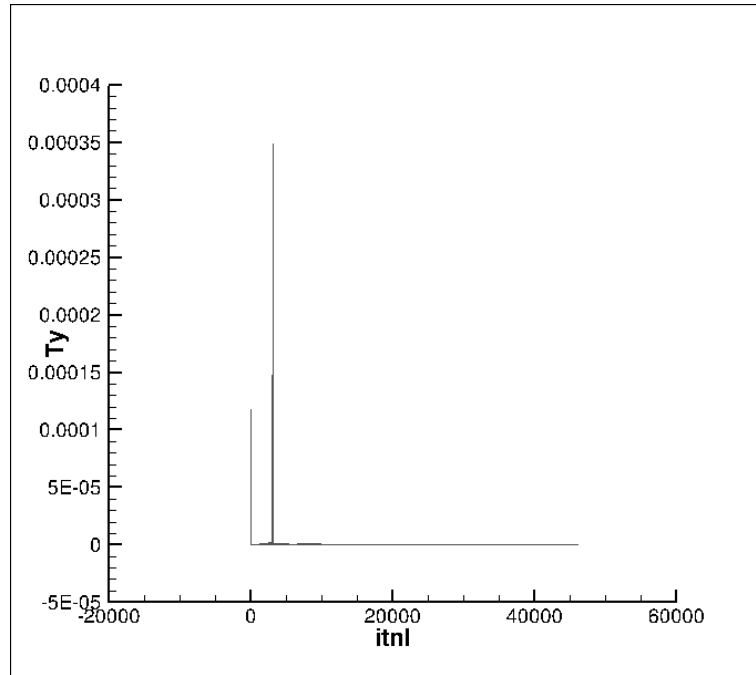


Figure 4: Differences in acceleration between non-linear iterations

Then we run the simulation without any stabilisation procedure with the added mass coefficient set to zero.The below figure,5 shows the evolution of forces for with and without the special stabilisation procedure

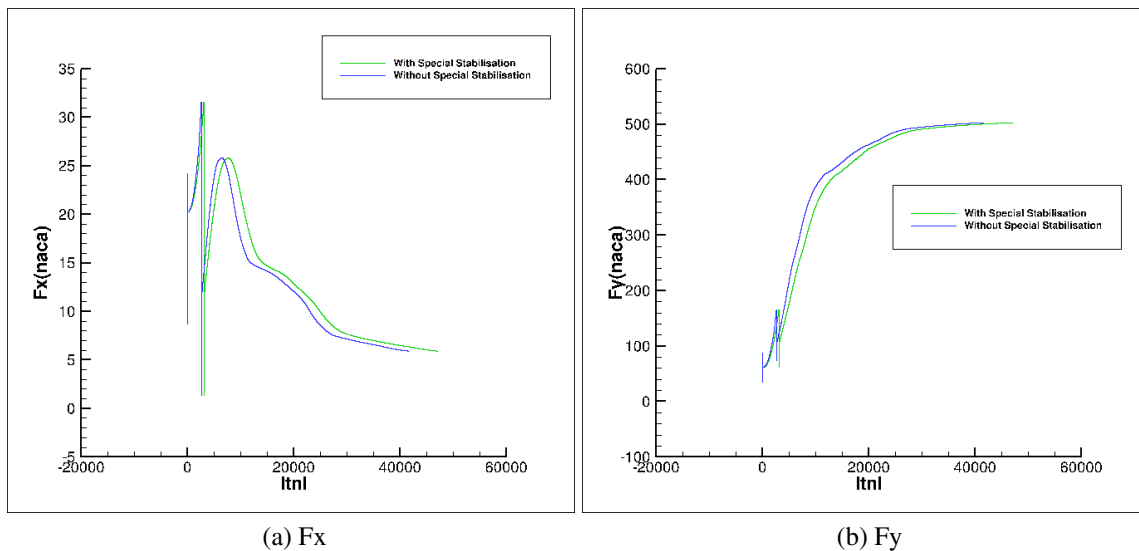


Figure 5: Comparison of Forces for with and without special stabilisation

It can be observed that, Forces in both the cases converge to a similar value. With the stabilisation procedure, the evolution of the forces are slowed down by a small amount. This is because of the densities considered, so there won't be any instabilities and it is not needed to apply the stabilisation procedure.

The below figure, 6 shows the comparison of the evolution of forces between Rigid motion and Weighting deformation technique.

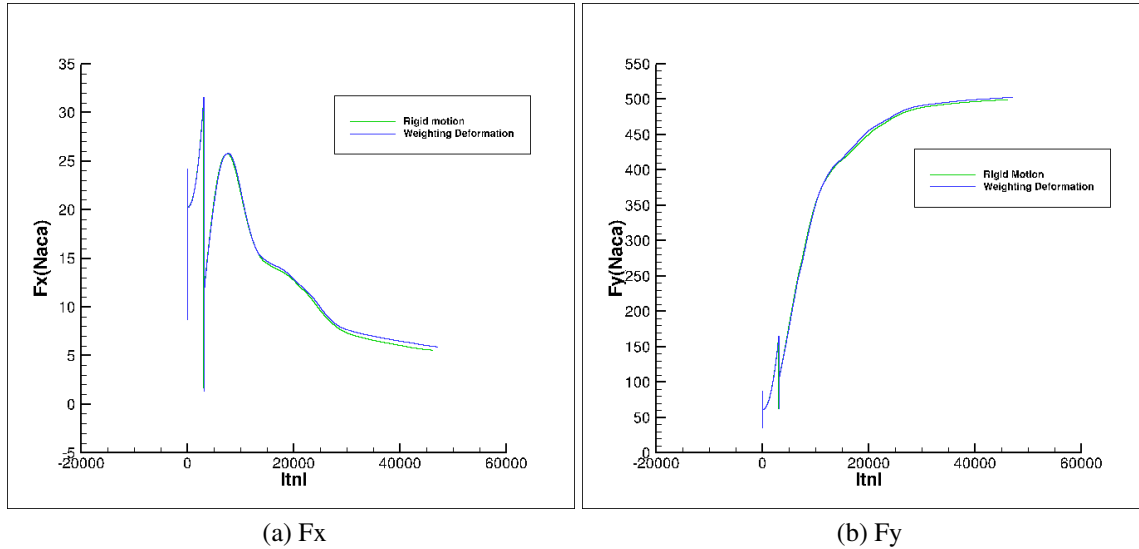


Figure 6: Comparison of Forces for Rigid and weighting deformation

The below figure, 7 shows the comparison of T_y position for the Rigid motion and Weighting deformation. At the smaller displacements, the two solutions are almost same, but as the displacement progresses, small variations can be observed. As small displacement of $0.25c$ was considered along T_y , the solutions doesn't show much of a difference.

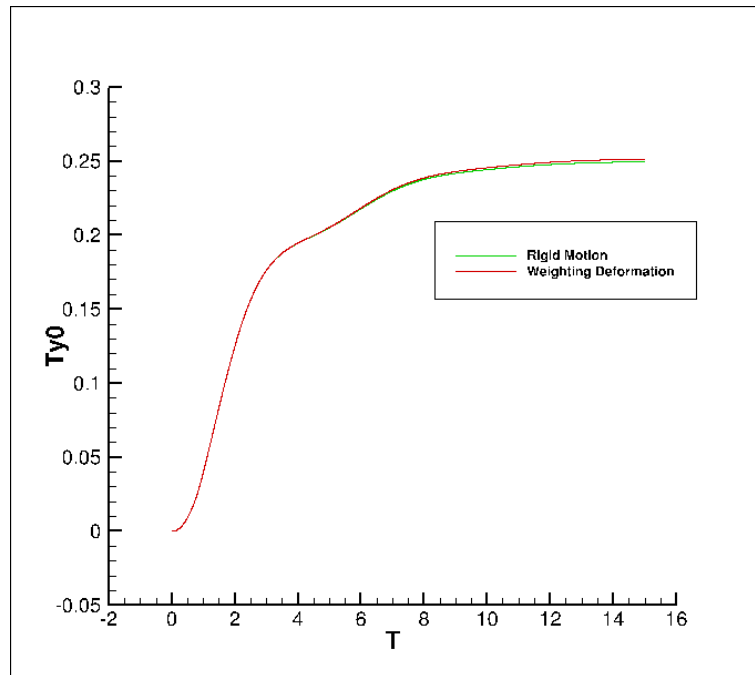


Figure 7: Comparison of Rigid and weighting deformation on T_y

1.2.2 Case 2 :Solid Density equal to 1/2 times the fluid density

In this case the Solid density is 1/2 times the fluid density. The mass of the wing is 40 kg/m.

First, we are going to study what happens when a special stabilisation is not used, the added mass coefficient was set to zero and the simulation was performed. It can be seen that within 7 non-linear iterations, the force starts to rise to a large value. The below figure.8 represents the evolution of forces for the same.

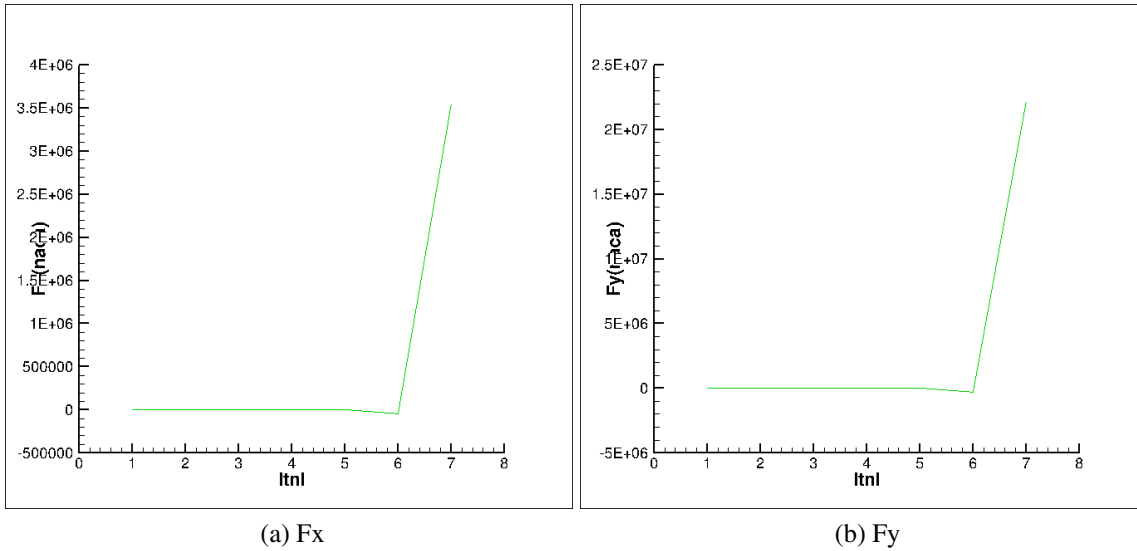


Figure 8: Evolution of forces without any stabilisation procedure

Now, We change the added mass coefficient estimation mode to approximate and it is computed only at the beginning and then simulation is performed. The below figure.9 shows the evolution of forces for this case and it can be that the forces are stable.

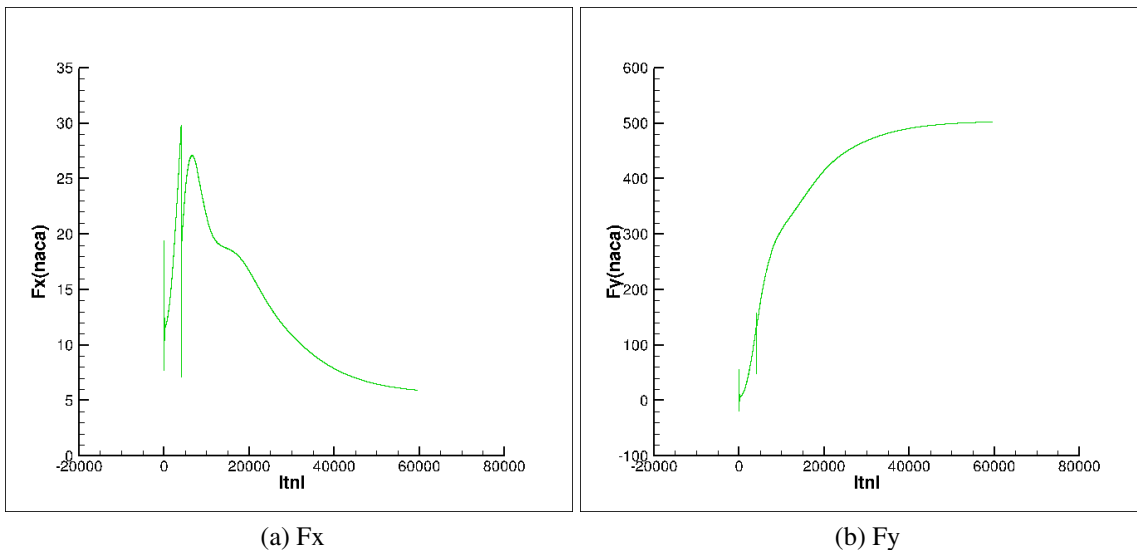


Figure 9: Evolution of forces with stabilisation procedure

Now, We impose suddenly a vertical acceleration and then calculate the added mass coefficient. We compare these values to the analytical values obtained for a flat plate. We performed a simulation by fixing the T_x motion and imposing a sudden vertical acceleration in y direction. We get the following the evolution of forces as shown in below figure.10

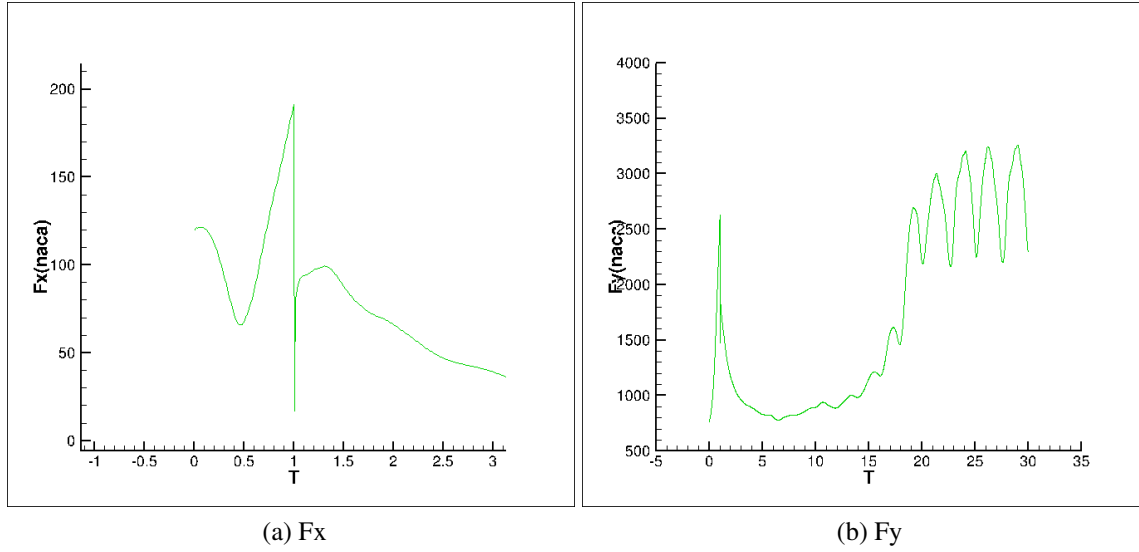


Figure 10: Evolution of forces for suddenly imposed vertical acceleration

Let's calculate and compare the results,
Analytically calculated added mass,

$$m_a = \rho \pi a^2$$

$$m_a = 1000\pi\left(\frac{1}{2}\right)^2$$

On calculating, we get $m_a = 785.5 \text{ kg/m}$ Then, added mass coefficient = $\frac{m_a}{m} = 19.6$

Simulated added mass,

$$\delta F_y = -M_{yy} * \delta A_y$$

$$1850 - 2625 = -M_{yy} * 1$$

$$M_{yy} = 750 \text{ N}$$

Added mass coefficient = $\frac{M_{yy}}{m} = \frac{750}{40} = 18.75$.

Thus, analytical results and numerical results are in close agreement. It can also be observed that the added mass component along the direction of the motion is much greater in this case.

The effect of added mass coefficient is set for a large value of 200. The below figures.11 represents the evolution of the forces for the same. It can be seen for the lower order of iterations the forces in the x direction decreases rapidly and goes to negative. But, then stabilises to value.

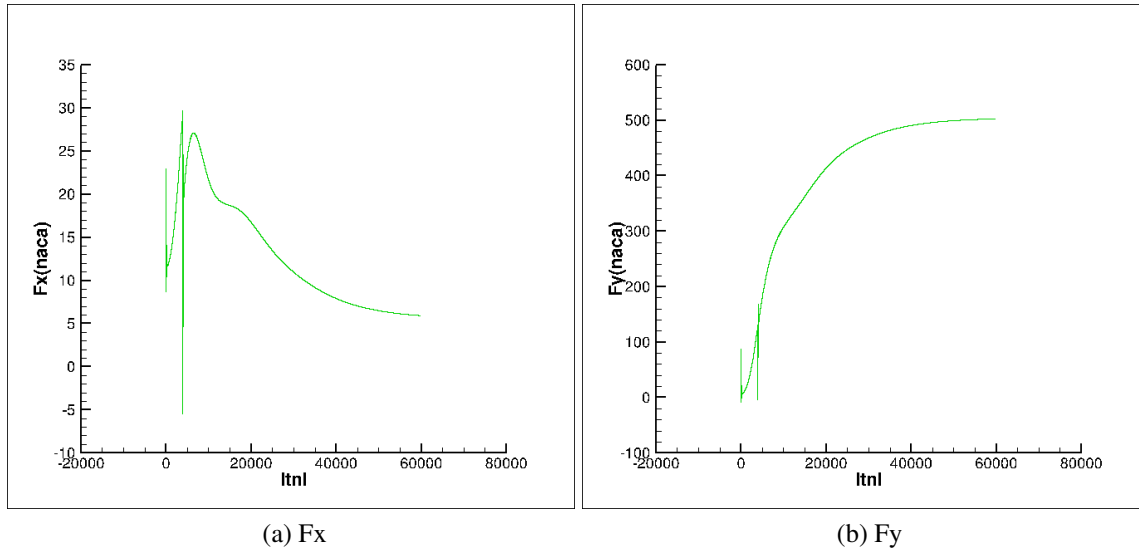


Figure 11: Evolution of forces

We now examine the frequency of the oscillation of the airfoil when it is released with some initial vertical displacement with the fluid at rest. The T_y is set to solved and the T_x is set to fixed. The below figure.12 shows the evolution of T_y with time.

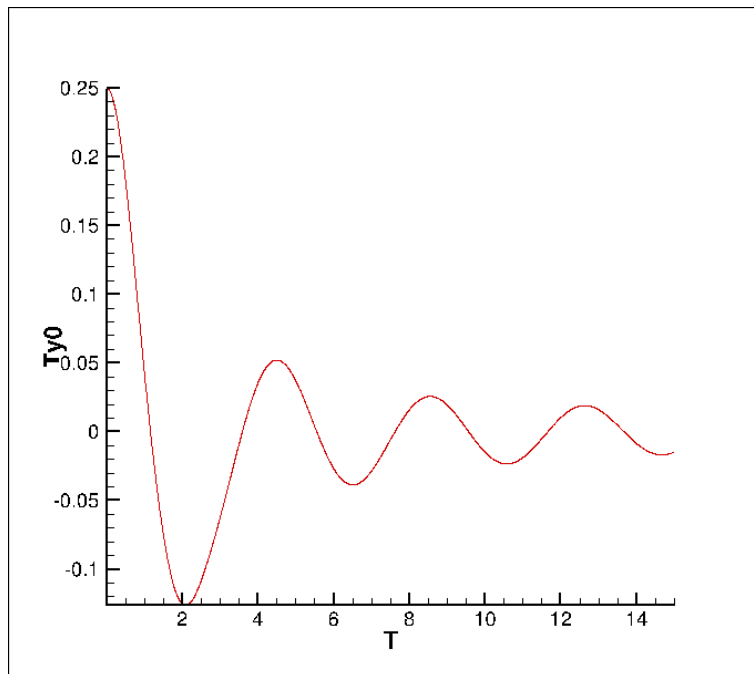


Figure 12: Evolution of T_y with time

We observe that the time period for the variation is about 4.2 sec. Then, we get the frequency as $f_{num} = 0.23809Hz$.

Now, if we consider the natural frequency of the wing, we have:

$$f = \frac{1}{2\pi} \sqrt{\frac{k}{m}} = 1.125Hz$$

Thus, We see a large difference from the numerical result. But, this is expected since the natural frequency of the mechanical system does not take into account the added mass effect. When we consider the added mass effect into consideration, we would have the natural frequency as:

$$f = \frac{1}{2\pi} \sqrt{\frac{k}{m + m_a}} = 0.25332Hz$$

This is more in agreement with the numerical results.

2 Part II:Use of CFD software for a classical resistance case

In this section,we are going to work on classical resistance configuration used for the CFD workshop Tokyo 2005,named case 1.3,related to the bare hull Frigate DTMB5415 as shown in the below figure 13.



Figure 13: DTMB case 1.3

The experimental conditions and results are presented below:

*Towing condition is still water

*Trim and sinkage free

*Bare hull without rudder

*Froude Number $F_n = \frac{U}{\sqrt{g.L_{pp}}} = 0.28$

*Reynolds Number $R_e = \frac{U.L_{pp}}{\nu} = 1.26e7$

where, U is ship speed

L_{pp} length between perpendiculars

g gravitational acceleration

ρ density of water

ν kinematic viscosity

*Experimental resistance coefficient

$$C_T = \frac{R_T}{0.5\rho U^2 S_0} = 4.23e-3$$

where, R_T is total resistance

S_0 is the wetted surface at rest

When Dynamic Equilibrium is reached,

-Sinkage $T_{z0} : -1.82e-3 L_{pp}$

-Trim $R_{y1} : -0.108 deg$

The simulation was setup using C-wizard which automatizes the mesh generation and the input parameters for this classical resistance case. Given CAD geometry of the hull was imported. Then, the half of the body is taken as the input. The Body orientation is set as CoG to bow towards negative X-axis and Cog to side towards positive Y-axis. The body is aligned with Cartesian axis. It is important to specify all these information because it is important to specify the orientation and the center of gravity to get accurate results. The body mass and center of gravity is computed automatically. Then the additional input parameters are defined and also mesh setup is completed. Then the mesh is manually checked. Then the solving is done with the help of a supercomputer LIGER. The results are then post-processed and studied.

The below figures.14 represent evolution of forces F_x, F_z . Enough forces are taken to ensure the forces are converged at the dynamic equilibrium. F_x represents the resistance force against movement of the ship and F_z represents the upward buoyancy force exerted by the water against the ship body.

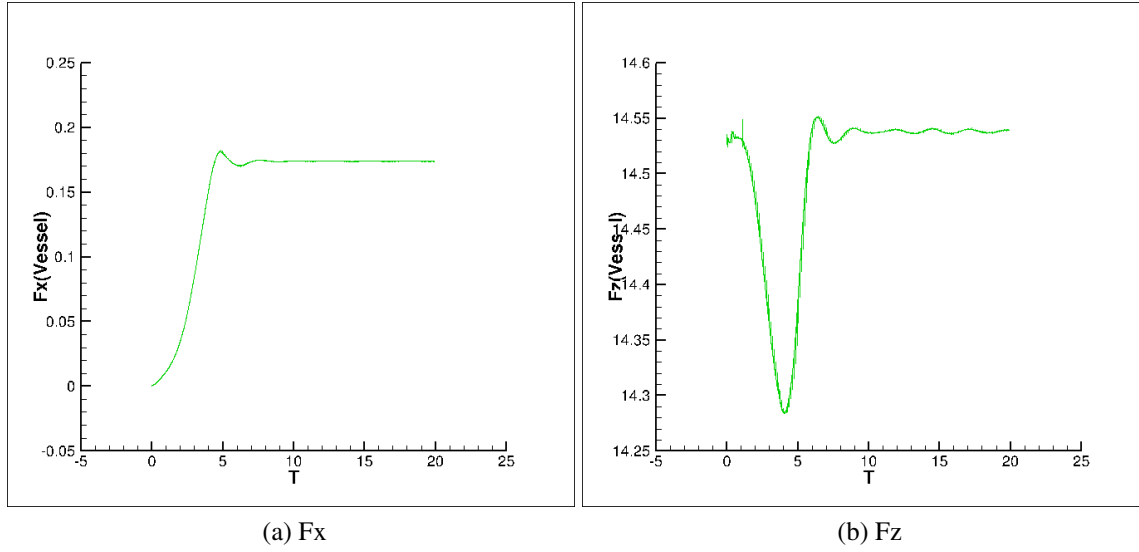


Figure 14: Evolution of Force

The below figures.15 and 16 represents the M_z , evolution of acceleration of the hull in the z-direction and acceleration of y-axis rotation. As it is a quasi-static approach, a guess of new equilibrium is computed periodically. After the relaxation, the new shape is applied through an imposed deformation within the given time. This can be observed in the graphs.

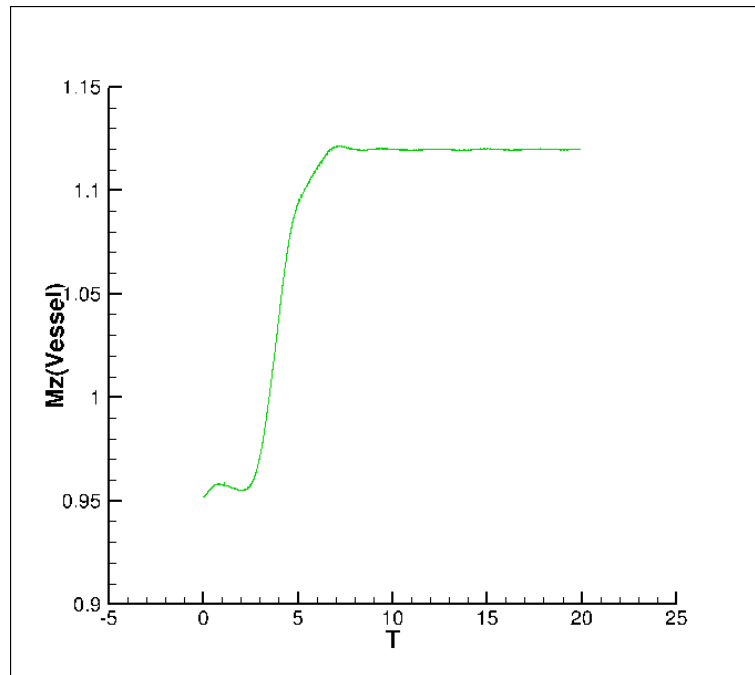


Figure 15: Evolution of M_z

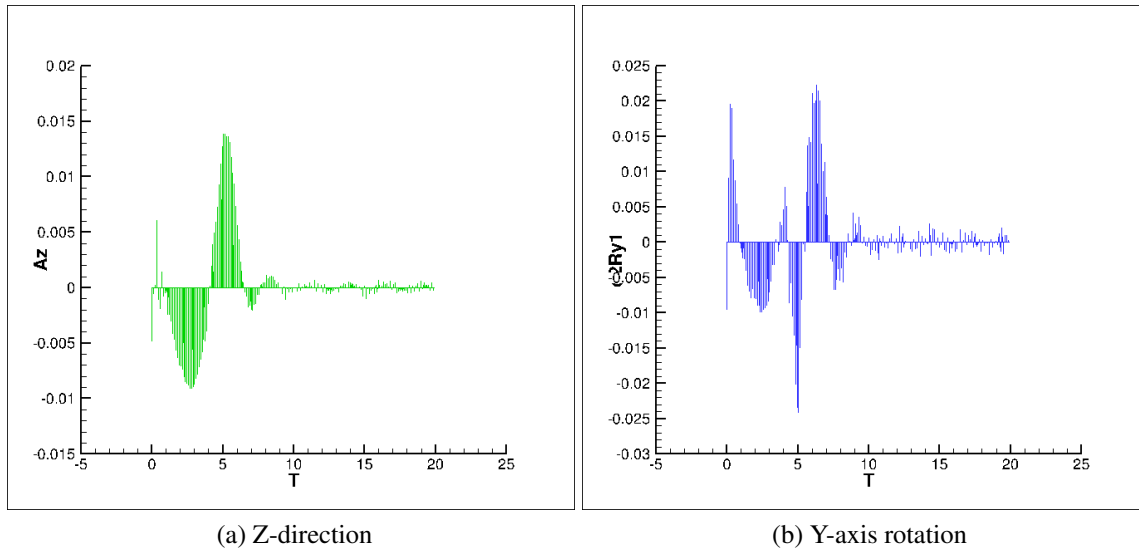


Figure 16: Evolution of Acceleration

The evolution of residuals of velocity components, turbulent kinetic energy and the pressure field is shown in the figure 17,18 and 19. There can be observed a rise and then drop of the residuals which represents the non linear iterations taking place at each time step.

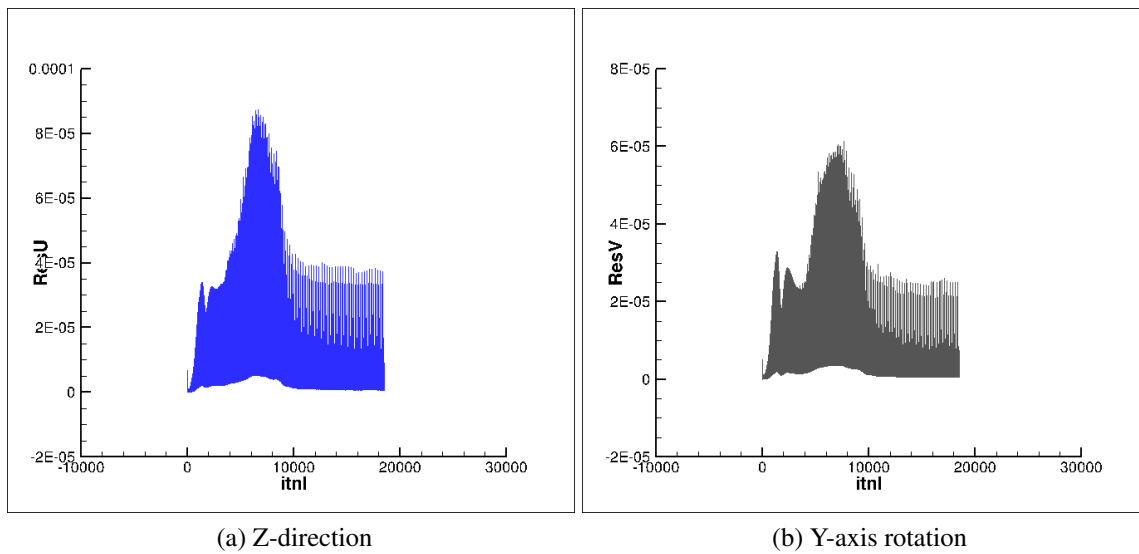


Figure 17: Evolution of Residual U and V

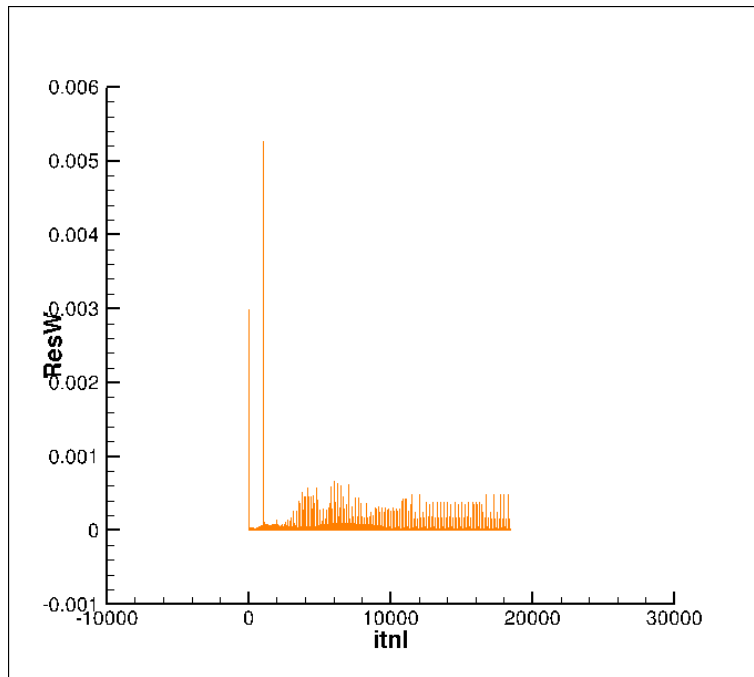


Figure 18: Evolution of Residual W

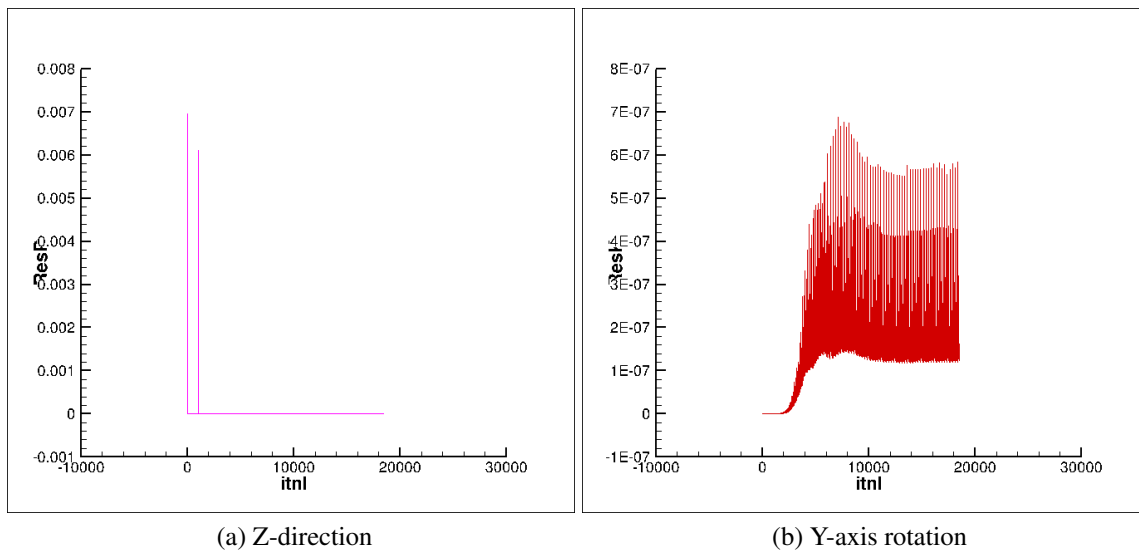


Figure 19: Evolution of Residual P and K

2.1 Evaluation of Trim, Sinkage and Resistance Coefficient

This section is dedicated to compute the numerical results for the trim, sinkage and the resistance coefficient and compare them with the experimental results.

2.1.1 Trim

The figure 20 indicates the evolution of rotation of c.g. along y axis until dynamic equilibrium. Trim is then computed as the net change in orientation after reaching the dynamic equilibrium

$$trim = R_{y1}(2) - R_{y1}(1)$$

where, $R_{y1}(2)$ is the angle at dynamic steady state, and $R_{y1}(1)$ at the initial state. From the figure, it was found that,

$$Trim = -0.0019774rad = -0.1133deg$$

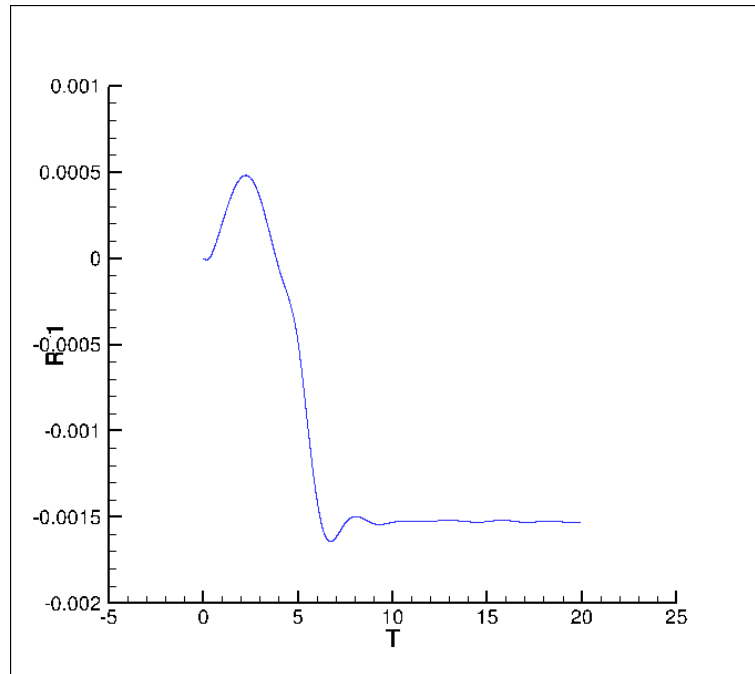


Figure 20: Evolution of Trim

2.1.2 Sinkage

The figure 21 indicates the evolution of displacement of c.g. along z-axis. Sinkage is then defined as the net displacement of c.g at dynamic equilibrium from its initial position.

$$Sinkage = T_{z0}(2) - T_{z0}(1)$$

where, $T_{z0}(2)$ is the position at the dynamic steady state, and $T_{z0}(1)$ at the initial state. From the figure, it was found that,

$$sinkage = -0.001785$$

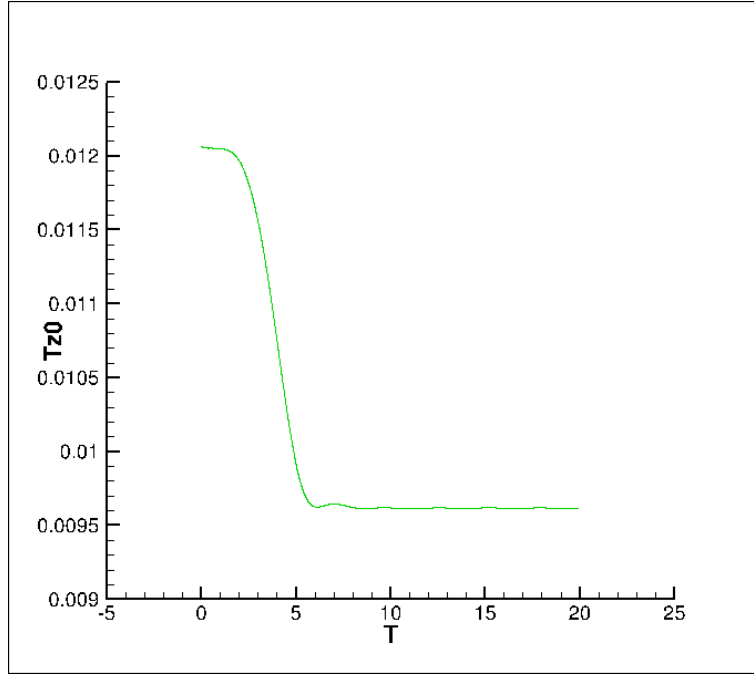


Figure 21: Evolution of Sinkage

2.1.3 Resistance Coefficient(C_T)

Resistance coefficient is defined as follows:

$$C_T = \frac{R_T}{0.5\rho_{water}U^2S_0}$$

$F_x = 0.122N$ The total wetted area was estimated as, $S_0 = 0.148524units$ Therefore, $C_T = 0.00425$

The below table summarises the numerical results and compares it with the experimental results. It can be observed that the trim, sinkage and resistance coefficient are in agreement with the experimental results.

Parameter	Numerical results	Experimental results
Trim, R_y	-0.1133	-0.108
Sinkage, T_{zo}	-0.00178562	-0.00182
Resistance coefficient, R_T	0.00425	0.00423

Table 2: Comparison of Trim, Sinkage and Resistance coefficient

2.1.4 Analysis of free surface elevation along the hull

The below figure,22 represents the comparison between the numerically computed free surface elevation and the experimental results for the same along the hull. The results obtained are in good agreement with the experimental results.

ISIS-CFD used an interface capturing technique. So, a very fine grid with very small cell size height close to the interface is essential to capture the interfaces sharply. But, this type of method is reliable if the grid preserves a sufficient density of points to describe the interface of discontinuity. Thus, it is important to maintain dynamically a prescribed density of points for a fine grid close to the evolving interface to capture it sharply void of any dispersion.

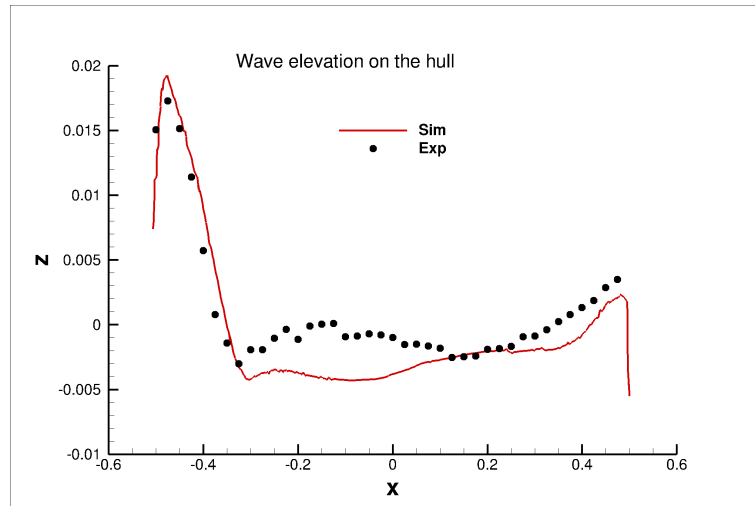


Figure 22: Comparison free surface elevation

2.2 Visualisation of flow

The below figure,23 shows the visualisation of the free surface wave elevation.

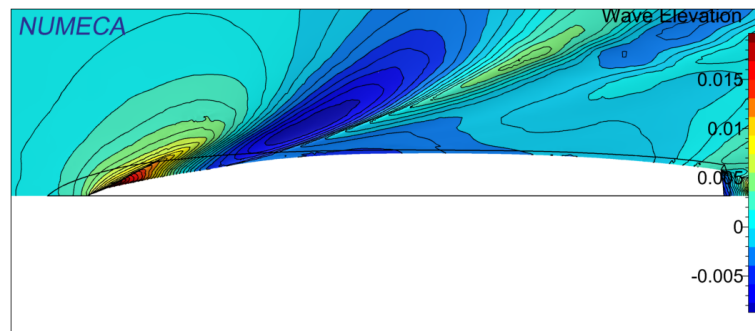


Figure 23: Visualisation of free surface wave elevation

2.3 Euler vs RANSE simulation

The below figures.24,25 and 26 represents the M_z , evolution of acceleration of the hull in the z-direction and acceleration of y-axis rotation for the Euler method. It can be observed that the F_x changes and there are small fluctuation in the acceleration of the hull in the z-direction A_z at the beginning .

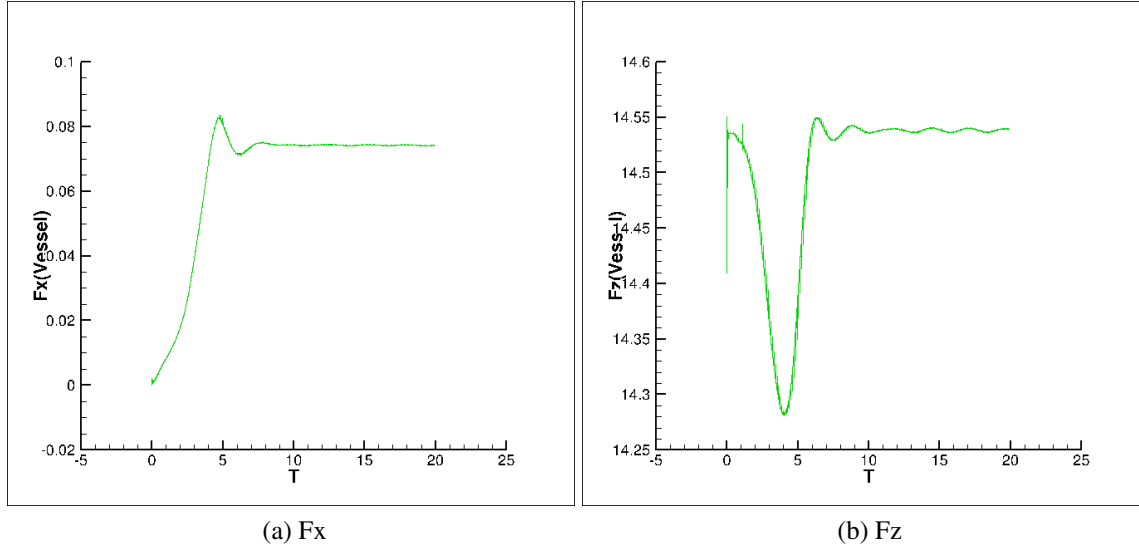


Figure 24: Evolution of Force

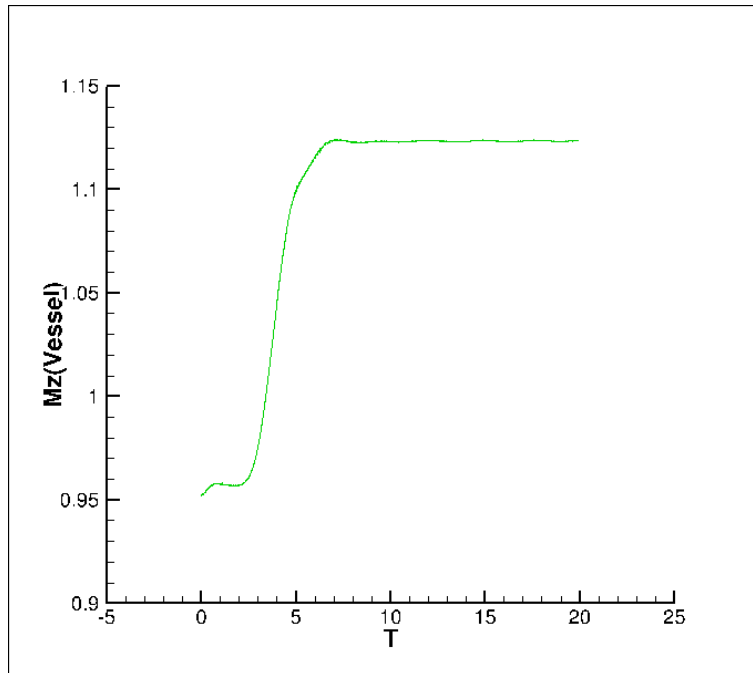


Figure 25: Evolution of M_z

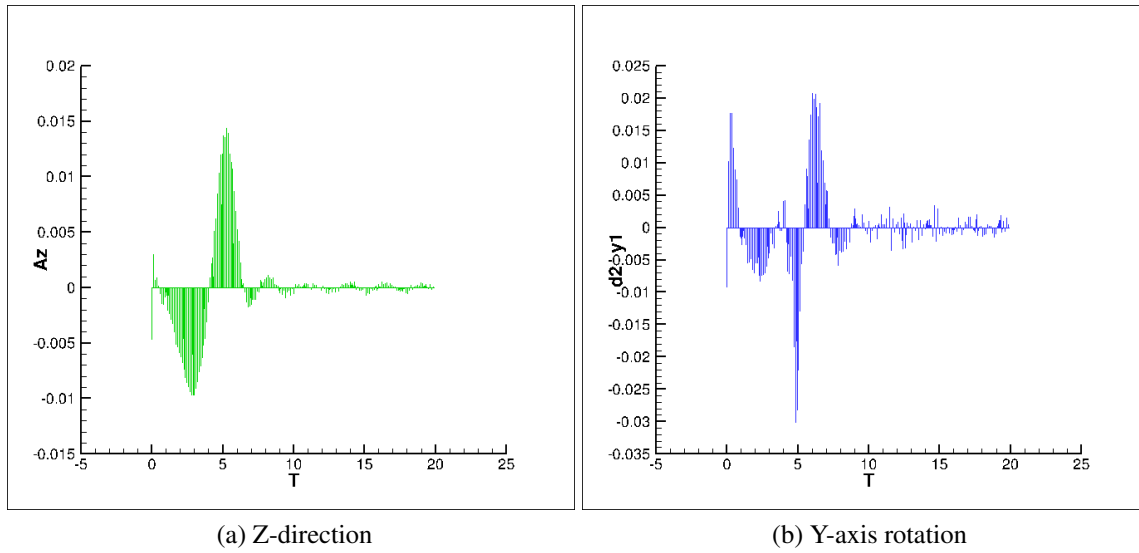


Figure 26: Evolution of Acceleration

2.4 Quasi-static approach vs Resolution of the Newton law

The below figures 27, 28 and 29 represent the M_z , evolution of acceleration of the hull in the z-direction and acceleration of y-axis rotation for the Resolution of Newton method. With the implementation of the Newton method, changes can be observed in acceleration along the hull in the z-direction and also in acceleration of y-axis rotation. There are less fluctuations in these graphs because in comparison in the quasi-static approach where a guess of new equilibrium is computed periodically. After the relaxation, the new shape is applied through an imposed deformation within the given time which is not the case in the Newton approach.

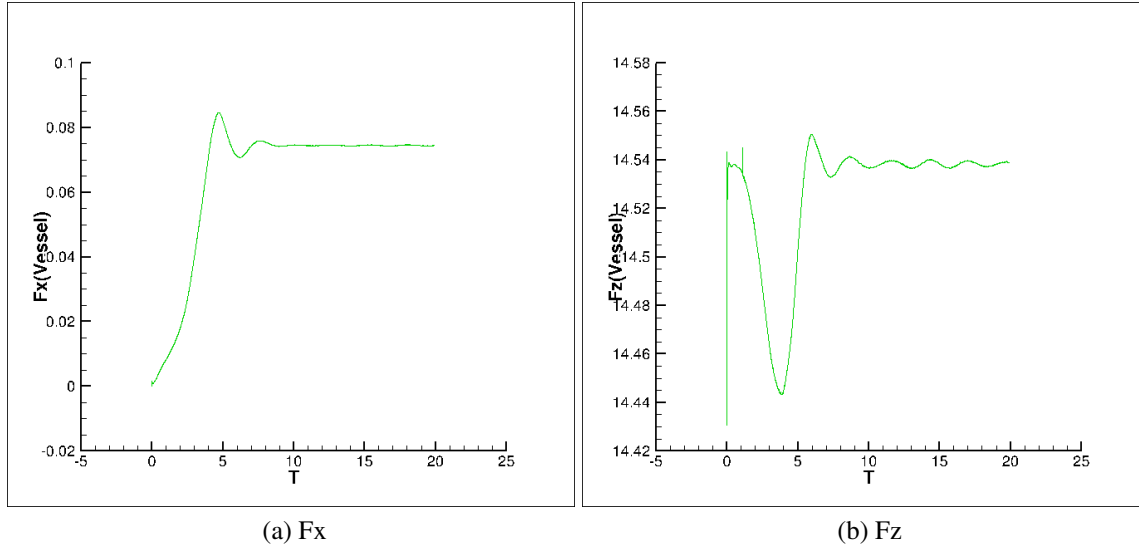


Figure 27: Evolution of Force

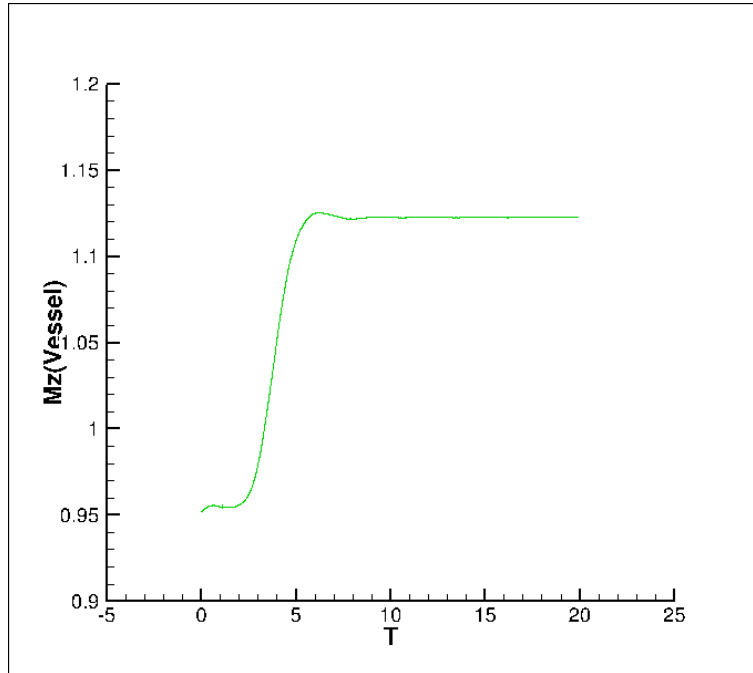


Figure 28: Evolution of M_z

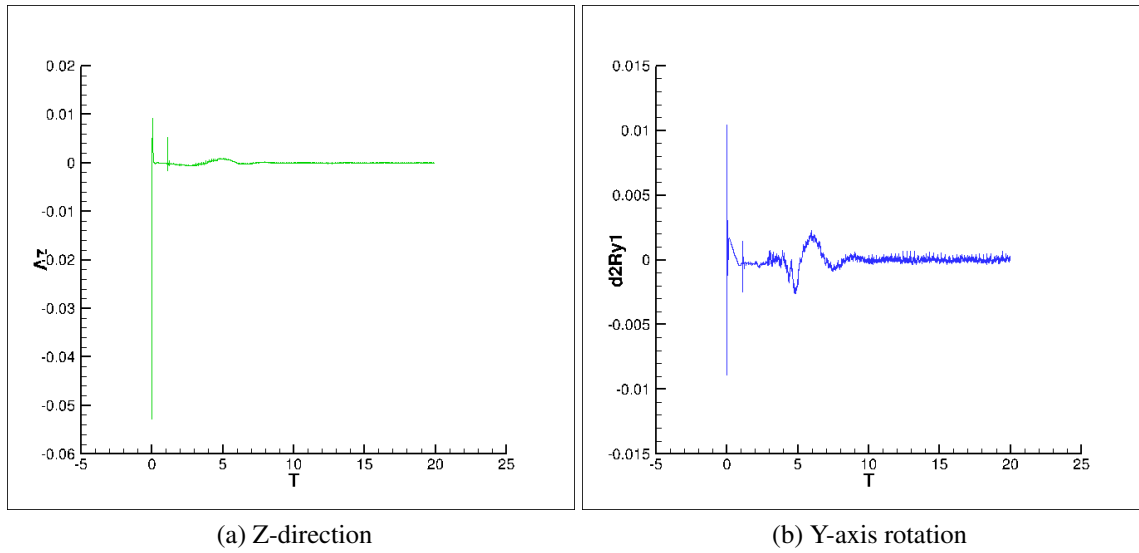


Figure 29: Evolution of Acceleration

3 Part III :Study of a 3D Composite Plate through a modal approach

In this section,we are going to study the 3D composite plate.It corresponds to a composite flat plate (span=0.3048m,cord=0.0762m,thickness=0.804e-3).A ISIS-CFD modal file had been generated using the abaqus software.This modal file was given as an input for the fluid solver.

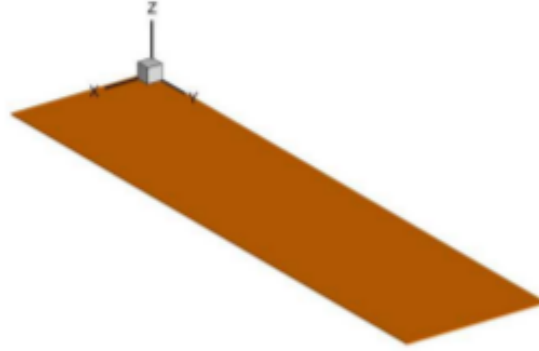


Figure 30: Evolution of F_x

In this study,Simulations are performed using a quasi-static approach instead of solving the dynamic modal equations.This enables to gain CPU time while exploiting a possible large time step,a first order temporal scheme,a limited non-linear gain.Six cases of simulations were ran and analysed.For Velocity,10m/s and 20m/s and degrees 2,6 and 10.All the cases are for the $[+45/0]_s$.

The below figures 31,32,33,illustrates the evolution of forces for all the cases considered.It can be observed that the lateral (F_z) component is higher in comparison with other two components.When the angles of attack or at higher velocity,the fluid forces oscillate in reaction to the structure's oscillations but then due to damping they eventually reach a static equilibrium.

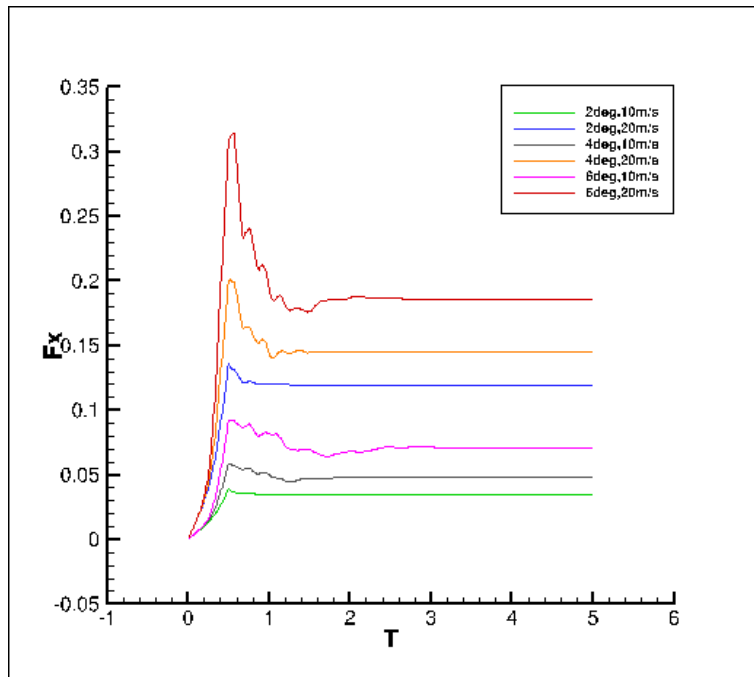


Figure 31: Evolution of F_x

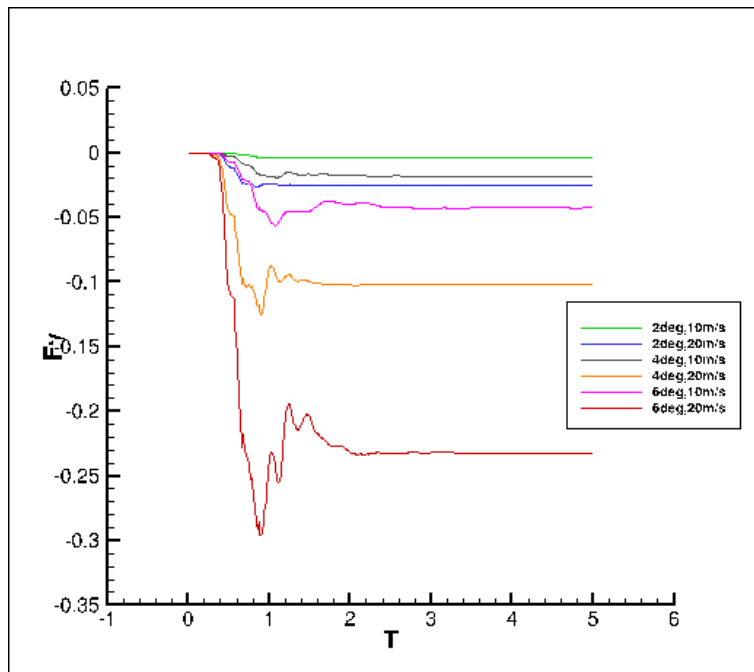


Figure 32: Evolution of F_y

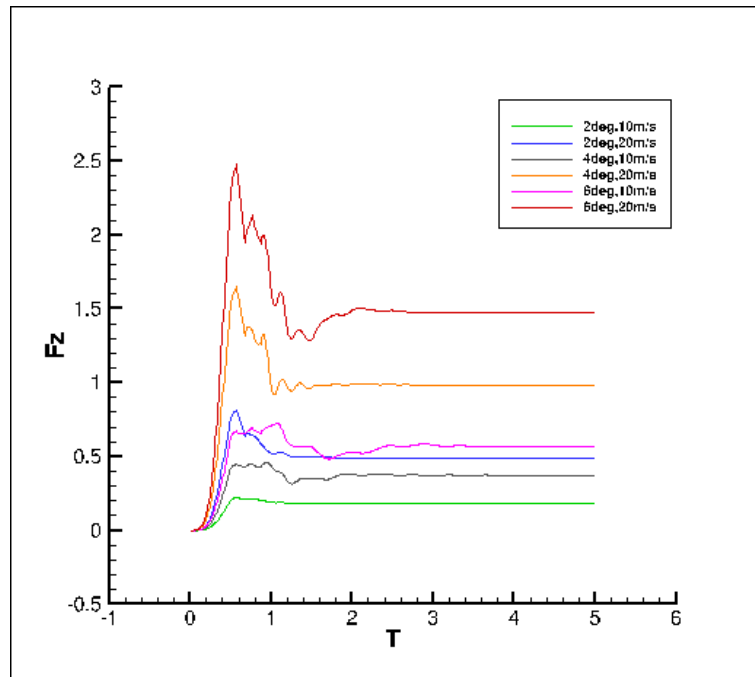


Figure 33: Evolution of F_z

The below figure 34,35 and 36,illustrates the evolution of displacement for all the cases.As the consequence of force being in the Z-direction,We can observe large deflections in comparison with the other two components.Large angles of attack and higher velocity create more oscillations in the beginning which are then damped,and have a larger static tip deflections.

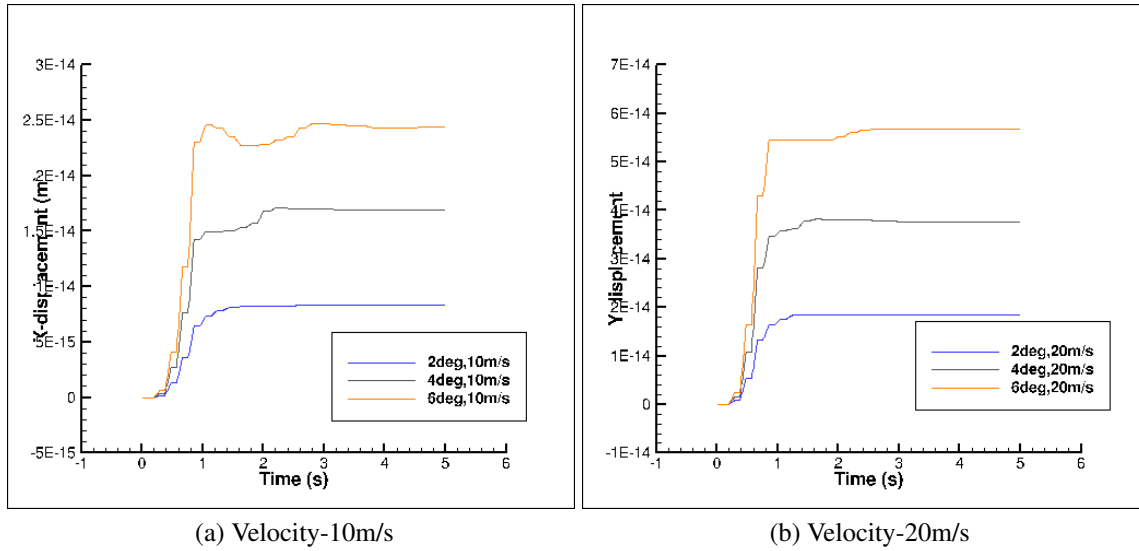


Figure 34: Evolution of X-displacement

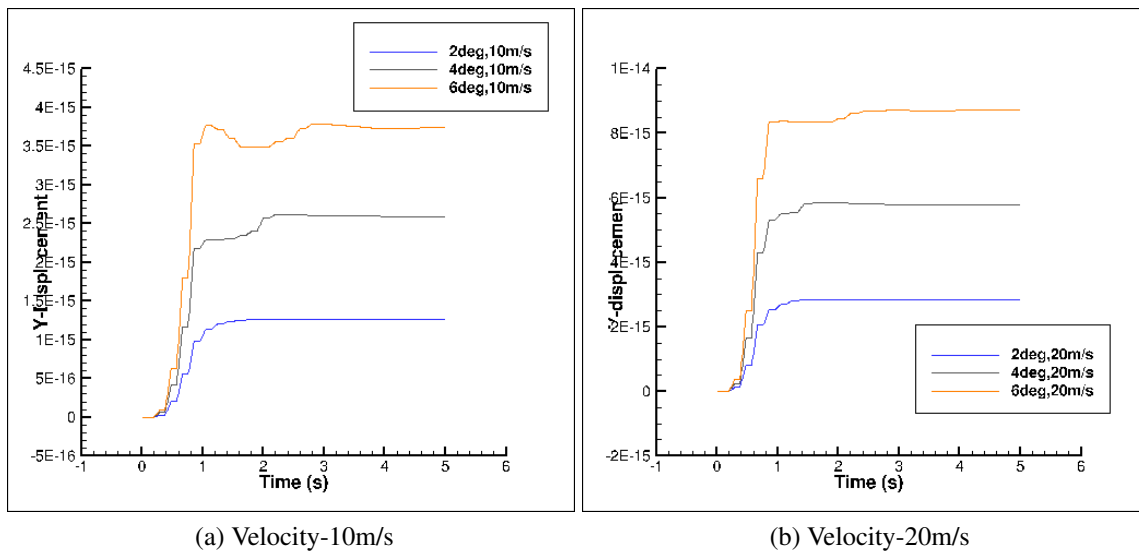


Figure 35: Evolution of Y-displacement

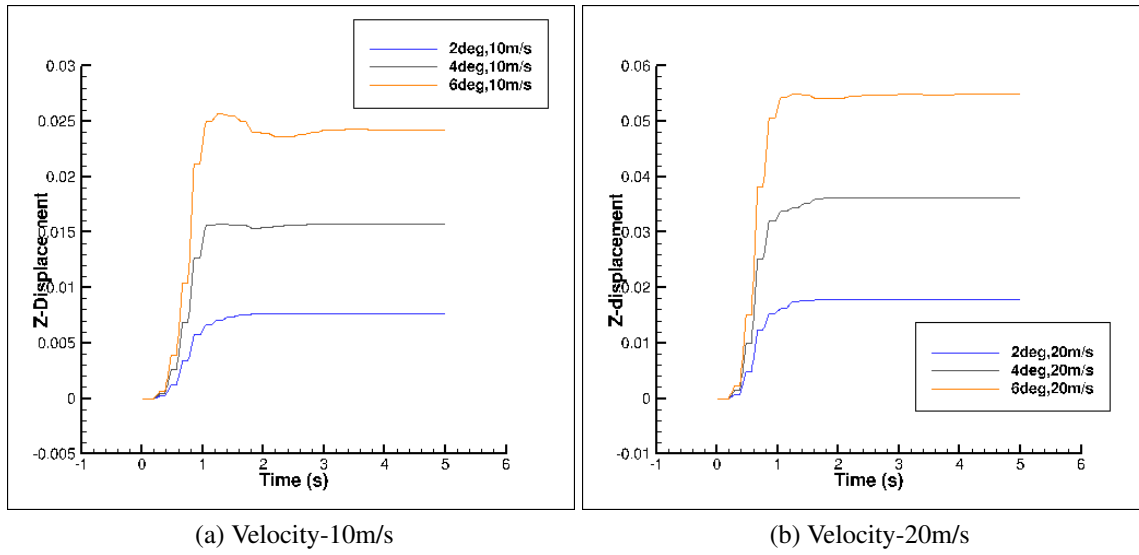
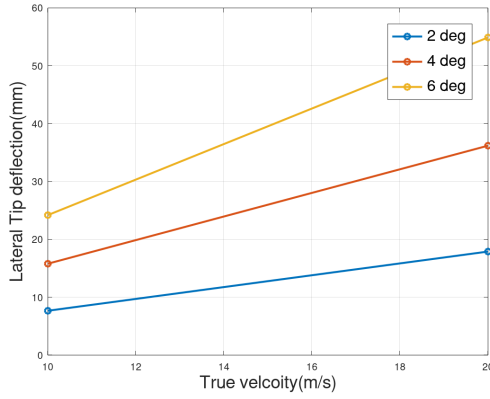


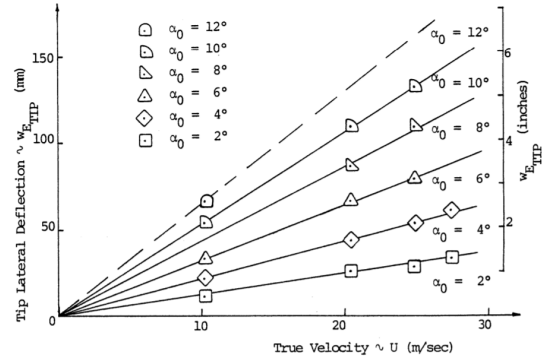
Figure 36: Evolution of Z-displacement

3.1 Lateral deflection of the tip

The lateral deflection was compared with the experimental values. The below image.37 represents the value of lateral tip deflection for all cases considered. When compared with the experimental values, it showed good agreement with experimental values.



(a) Simulated result



(b) Experimental result

Figure 37: Comparison of Lateral deflection with experimental values

As not enough time was available to go in this validation work. I couldn't explore the flutter phenomenon and observe the evolution of the flow fields at sections along the plate during flutter. so, I would like to explore this phenomenon.